Journal of Photochemistry & Photobiology A: Chemistry 368 (2019) 227–232

Contents lists available at ScienceDirect

Journal of Photochemistry & Photobiology A: Chemistry

journal homepage: www.elsevier.com/locate/jphotochem

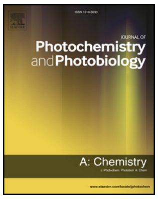

Improved photocatalytic activity of rutile TiO_2 for organic oxidation through Ag nanoparticles and borate anions

Jianjun Zhao, Bangde Luo, Xianqiang Xiong, Xiao Zhang, Yiming Xu*

State Key Laboratory of Silicon Materials and Department of Chemistry, Zhejiang University, Hangzhou, 310027, PR China

ARTICLE INFO

Keywords:
Rutile
Silver
Borate
Photocatalysis
Phenol oxidation
Charge transfer

ABSTRACT

Rutile TiO_2 (RT) is usually used as photocatalyst for water oxidation, but seldom for organic oxidation, probably due to the slow reduction of O_2. Herein we report a mutual effect of Ag nanoparticles and borate anions greatly increasing the photocatalytic activity of RT for phenol oxidation in neutral aqueous solution. RT was homemade, followed by calcination at 200—800 °C. With a given RT, the rates of phenol oxidation on the addition of Ag and borate were increased and decreased, respectively. In the presence of both Ag and borate, interestingly, the rate of phenol oxidation was larger than that in the presence of Ag. A (photo)electrochemical measurement revealed that Ag and borate, in contact with the irradiated RT, could catalyze O_2 reduction and phenol oxidation, respectively. Since the electron and hole transfer processes would promote each other, the positive effect of Ag is further enhanced in the presence of borate. This work demonstrates that RT could be developed as a promising photocatalyst for organic oxidation through a surface co-catalyst.

1. Introduction

Semiconductor photocatalysis has attracted great attentions for energy and environmental use. Among various photocatalysts, TiO_2 is the most studied, mainly due to its low cost, good activity, and high stability [1–4]. However, the system efficiency is still not high enough to enable practical application. For instance, the quantum yield of phenol oxidation in the aqueous suspension of P25 TiO_2 (a mixture of anatase and rutile) is only 0.14 at 365 nm [5]. It is widely recognized that the primary process occurring on the irradiated TiO_2 is generation of the electrons (e_{cb}^-) and holes (h_{vb}^+) in the conduction and valence bands, respectively. These charge carriers then recombine to heat, or migrate onto the surface reacting with suitable sorbents. Apparently, to improve the efficiency of TiO_2 photocatalysis, one needs not only to increase the number of e_{cb}^- and h_{vb}^+ reaching the oxide surface, but also to accelerate the interfacial charge transfer to target reactants.

There are many factors that influence the photocatalytic reactions of TiO_2 [6,7]. A common factor is the calcination temperature (T_s) of TiO_2 precursors, which not only determines the crystal structures, but also changes the physical parameters of TiO_2. In our impression, rutile TiO_2 (RT) and anatase TiO_2 (AT) are often used as photocatalysts for water and organic oxidation, respectively. This is probably due to the adsorption and reduction of O_2 on RT in water that are weaker and slower than those on AT, respectively [8]. In aqueous solution at pH 0, the conduction band edge potentials for AT and RT are about −0.12 and 0.06 V versus normal hydrogen electrode (NHE), respectively [2,9], whereas the redox potentials for the O_2/HO_2 and O_2/H_2O_2 couples are −0.05 and 0.70 V (NHE), respectively [10]. This allows the one-electron reduction of O_2 to occur only on AT. However, the valence band edge potentials of AT and RT are similar. Then RT might be developed as a promising photocatalyst for organic oxidation, if the slow reduction of O_2 is overcome. First, the apparent activity of TiO_2 greatly changes with its physical parameters, including crystal structures and surface area [6–8]. But the intrinsic activity of TiO_2 exponentially increases with the increase of T_s, regardless of the solid structures in the forms of AT, RT, brookite, and their mixture [8,11–14]. A high intrinsic photocatalytic activity of TiO_2 means a large number of e_{cb}^- and h_{vb}^+ available to reactants on the oxide surface. Second, RT has a thermal stability much higher than those of AT and brookite, respectively. Then RT can be prepared at high T_s, without problem in phase transformation. By using a co-catalyst, it is highly possible to exploit the high intrinsic photocatalytic activity of RT, reserved at high T_s. For example, the Ag nanoparticles (NPs) deposited on the surface of RT (devoted as Ag/RT) can increase the rate of dye photodegradation in water, ascribed to the Ag NPs that trap e_{cb}^-, and hence accelerate O_2 reduction [15,16]. But the effect of T_s on the photocatalytic activity of Ag/RT has not been found yet in the literature. On the other hand, it have been reported that borate anions present in the aqueous suspensions of AT

---

* Corresponding author.
E-mail address: xuym@zju.edu.cn (Y. Xu).

https://doi.org/10.1016/j.jphotochem.2018.09.045
Received 14 July 2018; Received in revised form 30 August 2018; Accepted 25 September 2018

and brookite can promote phenol degradation, respectively [17–19]. But the borate effect on the RT-photocatalyzed reaction has not been examined. Since inorganic anions such as borate are widely present in aquatic environment, the anions effect on the photocatalytic degradation of organic pollutants needs to be examined [20]. Moreover, the Ag NPs deposited on AT also show an excellent antimicrobial activity in the dark or under UV light [21]. These literatures encourage us to make a further study of Ag-containing RT for environmental use.

In this work, the effect of Ag NPs and borate anions on the RT-photocatalyzed reactions has been examined as a function of T_s. To do this, phenol was selected as a model substrate, and the reaction was carried out in neutral aqueous solution under UV light at wavelengths longer than 320 nm. Under such conditions, phenol photolysis in solution and its adsorption on TiO_2 were both negligible. Then the observed decrease of phenol concentration in aqueous phase under UV light would be only a result of RT photocatalysis. RT samples were prepared from the hydrolysis of $TiCl_4$, followed by calcination at different T_s. To ensure the same amounts of Ag used in different tests, a commercially available Ag NPs was directly added into the aqueous suspensions of RT, under magnetic stirring. It was observed that Ag NPs and borate anions had a positive and negative effect on the RT-photocatalyzed reactions, respectively. In presence of both Ag and borate, however, the rate of phenol oxidation was larger than that in presence of Ag. To understand the effects of Ag and borate, several experiments were performed, including the photocatalytic and electrochemical reduction of O_2, and the photoelectrochemical oxidation of phenol over a rutile film electrode.

2. Experimental section

2.1. Materials

N,N-diethyl-1,4-phenylenediamine (DPD), peroxidase (POD), azomethine H (AH), silver NPs, and methyl blue (MB) were purchased from Sigma-Aldrich, and other chemicals from Shanghai Chemicals Inc., China., including $TiCl_4$, $Na_2B_4O_7$ (borate) and phenol. RT was prepared by following the literature procedure [22]. In brief, 40 mL of $TiCl_4$ was added dropwise to 1000 mL of 0.5 M HCl in an ice bath. Then the suspension was heated at 60 °C for 2 h. After storage overnight, the solid was collected by filtration, and washed thoroughly with distilled water, till no chlorides were present in the filtrate ($AgNO_3$ test). Finally, the powders were calcined at 200–800 °C in air for 3 h. The sample is denoted as RT*x*, where *x* represents the calcination temperature used.

2.2. Solid characterization

X-ray diffraction (XRD) pattern was recorded on a Rigaku D/max-2550/PC diffractometer. The average crystallite diameter (d_{XRD}) was estimated by using Scherrer equation. Diffuse reflectance spectrum was recorded on a Shimadzu UV-2550 with $BaSO_4$ as a reference. The reflectance (R) was transferred into the Kubelka—Munk unit, $F_R = (1-R)^2/(2R)$. Then the band gap energy of TiO_2 (E_g) was estimated with a Tauc plot [23], $(F_R E_{hv})^{0.5}$ vs. E_{hv}, or with a derivative method [24], $d\ln F_R/dE_{hv}$ vs. E_{hv}, where E_{hv} represents light energy. Photoluminescence (PL) spectrum was recorded on a Shimadzu F-2500 spectrophotometer, and the solid was excited at 325 nm. Adsorption-desorption isotherm of N_2 was measured at 77 K on an ASAP2020 apparatus. From the adsorption branch of the isotherm, the Brunauer-–Emmett–Teller surface area (A_{BET}), total pore volume (V_p), micropore volume (V_m), and the Barrett–Joyner–Halenda average pore size (d_p) were calculated. Scanning electron microscopy (SEM) measurement was performed on a Hitachi S-4800. Moreover, the surface area of RT in aqueous suspension (A_{MB}) was also estimated using an adsorption method [25]. First, the adsorption isotherm of MB on TiO_2 in aqueous solution at 25 °C and pH 6.5 was measured. Then by application of the Langmuir adsorption equation, the maximum amount of MB was obtained, and used to calculate A_{MB}, based on the flat area of 1.2 nm^2 per MB molecule.

2.3. Photocatalysis and analysis

Experiments were carried out in a Pyrex-glass reactor (50 mL), with a cooling water jacket at 25 °C. Unless stated otherwise, the condition was fixed at 1.00 g/L TiO_2, 0.43 mM phenol, and initial pH 7.0. After a stock solution of Ag NPs or borate was added, the suspension pH was adjusted to 7.0 with a dilute solution of NaOH or $HClO_4$. Then the suspension was sonicated for 5 min, and stirred for 1 h, and irradiated with a mercury lamp (300 W, Shanghai Yamin). At given intervals, 2.0 mL of the sample was withdrawn, filtered, and analyzed as follows.

Organics in the filtrate was analyzed by HPLC (high performance liquid chromatography) on a Dionex P680 (Apollo C18 reverse column, and 50% CH_3OH eluent). H_2O_2 in the filtrate was measured through a POD-catalyzed oxidation of DPD [26]. In brief, the filtrate in a cuvette was mixed with a solution of phosphate buffer, DPD, and POD. After 60 s, the solution absorbance at 553 nm was recorded on an Agilent 8451 spectrometer, and used to calculate the concentration of H_2O_2 by using a standard curve. Borate anion was analyzed through its complex with azomethine H [27]. The filtrate was mixed with a solution of acetate buffer and AH. After 90 min, the solution absorbance at 413 nm was recorded, and then used for the calculation of borate concentration.

2.4. (Photo)electronical measurement

The TiO_2 film electrode was prepared by using a doctor blade method [17,18]. A gel containing RT200 was coated onto indium-doped tin oxide substrate, followed by annealing at 500 °C for 3 h. After cooling, the glass was cut into pieces (exposed area = 1.0 cm × 1.0 cm), and used as working electrode. To deposit Ag, the TiO_2 film electrode was soaked in 1.0 mM $AgNO_3$, and irradiated with UV light for 10 min. Then the glass was rinsed thoroughly with water, and dried at 50 °C overnight. The (photo)electrochemical measurement was carried out in 0.5 M $NaClO_4$ on a CHI660E Electrochemical Station (Chenhua, Shanghai). A saturated calomel electrode (SCE) was used as reference electrode, a platinum gauze as counter electrode, and a 150 W Xenon lamp as light source.

3. Results and discussion

3.1. Solid characterization

The solid was characterized with several techniques, and the results are shown in Fig. S1—S4 of the supporting materials. All of RT samples displayed a XRD pattern in good agreement with that for standard rutile TiO_2 (PDF no. 21-1276). As T_s increased, the diffraction peaks became more intensive and acute. This is due to the growth of rutile crystallites, as confirmed by the average diameter of (110) rutile crystals (Table 1). Moreover, the unit cell volume of RT (0.0621 nm^3) remained nearly unchanged with T_s. The XRD pattern of Ag NPs also well matched that of metallic silver (PDF no. 03-0931). The average diameter of (111) Ag was estimated to be 5.32 nm. In the diffuse reflectance spectrum of RT, there was a strong absorption band at wavelengths shorter than 420 nm. By using a Tauc plot or derivative method [23,24], the band gap energy of RT (E_g) was estimated, which was 3.02 ± 0.02 eV for all of the samples (Table 1). The value of E_g was also confirmed by PL measurement. After excitation with UV light at 325 nm, RT showed emission peaks centered at 411, 419, 437, 450, 462, 468, 481, and 492 nm, respectively. The peak at 411 nm (3.02 eV) is due to the band-to-band emission, whereas other peaks at 419–492 nm (2.96–2.52 eV) may be assigned to the exciton recombination of e_{cb}^{-}-h_{vb}^{+}, plus phonon modes [28], and/or to the recombination of free h_{vb}^{+} with the trapped e_{cb}^{-} in oxygen vacancies within the band gap of rutile [28–30]. Moreover, after normalized with the intensity at 419 nm, all of PL